

1 **Environmental Stress Testing of Wafer-Level Al-Al Thermocompression Bonds: Strength and**  
2 **Hermeticity**

3

4 N. Malik<sup>a,b</sup>, E. Poppe<sup>b</sup>, K. Schjøberg-Henriksen<sup>b</sup>, M. M. V. Taklo<sup>c</sup>, and T. G. Finstad<sup>a</sup>

5

6 <sup>a</sup> Centre for Materials Science and Nanotechnology, University of Oslo, Oslo, Norway

7 <sup>b</sup> SINTEF ICT, Dept. of Microsystems and Nanotechnology, P.O. Box 124 Blindern, N-0314 Oslo,  
8 Norway

9 <sup>c</sup> SINTEF ICT, Dept. of Instrumentation, P.O. Box 124 Blindern, N-0314 Oslo, Norway

10

11

12 **Corresponding Author:**

13 Nishant Malik

14 Centre for Materials Science and Nanotechnology (SMN)

15 University of Oslo

16 P.O. Box 1048, Blindern

17 0316 Oslo

18 Norway

19

20 Email: [nishant.malik@smn.uio.no](mailto:nishant.malik@smn.uio.no), [nishantmalik1987@gmail.com](mailto:nishantmalik1987@gmail.com)

21 Phone: +47-46350668

22

23

24

25

26

27

28

29

30

31

32

33

34

35

36

37

38

39

40

41

42

43

44 **Abstract**

45  
46  
47  
48  
49  
50  
51  
52  
53  
54  
55  
56  
57  
58  
59  
60  
61  
62  
63  
64  
65  
66  
67  
68  
69  
70  
71  
72  
73  
74  
75  
76  
77  
78  
79  
80  
81  
82  
83  
84  
85  
86  
87

Hermeticity, reliability and strength of Al-Al thermocompression bonds realized by applying different bonding parameters have been investigated. Laminates of diameter 150 mm were realized by bonding wafers containing membrane structures to wafers with patterned bonding frames. The laminates were bonded applying a bond force of 36 or 60 kN at temperatures ranging from 300 to 400 °C for 15, 30 or 60 minutes. The hermetic properties were estimated by membrane deflection measurements with white-light interferometry after bonding. Reliability was tested by exposing the laminates to a steady-state life test, a thermal shock test, and a moisture resistance test. Bond strength was measured by shear test and pull tests. Laminates bonded applying a bond force of 60 kN at temperatures of 350 or 400 °C resulted in hermetic bonds. No significant change in membrane deflection was observed after the steady-state life test or the thermal shock test. However, a gross leakage was observed in 1–11% of the dies after exposure to the moisture resistance test. The maximum leakage rate (MLR) estimated from membrane deflection measurements was below  $10^{-11}$  mbar·l·s<sup>-1</sup> for all laminates. The measured average bond strength of dies from selected laminates ranged from 28 to 190 MPa.

88 **Introduction**

89

90 Micro electro-mechanical systems (MEMS), especially inertial sensors such as mechanical resonators,  
91 gyroscopes and accelerometers, have fragile parts which need to be sealed in a vacuum environment for  
92 high performance and a long life time. A controlled ambient pressure is required in these sensors because  
93 of their mechanical damping characteristics. MEMS absolute pressure sensors require a vacuum cavity as  
94 a zero pressure reference. Therefore, a hermetic package is an essential requirement for such environment  
95 sensitive MEMS devices.<sup>1</sup>

96

97 Metal thermocompression bonding is a promising technology for hermetic encapsulation of MEMS  
98 devices. Metals have lower gas permeability than other reported intermediate bonding materials, thus they  
99 allow narrower seal frames which will yield a significant reduction in die size.<sup>2</sup> Al is an attractive choice  
100 of metal due to its CMOS compatibility. Successful Al thermocompression bonding has been reported<sup>3-6</sup>,  
101 but reports about a combination of hermetic and reliability properties are missing.

102

103 Hermeticity testing is commonly done in accordance with MIL-STD-883 test methods. Due to shrinkage  
104 of the device packaging size below 0.05 cm<sup>3</sup>, rejection leak rates mentioned in MIL-STD-883 are no  
105 longer valid.<sup>7</sup> More stringent rejection rates for volumes below 0.01 cm<sup>3</sup> are given in MIL-STD-750E.  
106 Traditionally, hermeticity was determined by a gross bubble test along with a He fine leak test. Now,  
107 depending on the application, more sensitive and accurate hermeticity testing methods are available.  
108 Optical measurement of changes in membrane deflection, Fourier transform infrared spectroscopy (FTIR),  
109 Q-factor testing and residual gas analysis are some of the commonly applied hermeticity test methods.<sup>8</sup>  
110 Various reliability tests are performed for sealed MEMS devices to study the effect of various harsh  
111 environmental conditions relevant for the target application. Such tests are also mainly done in  
112 accordance with the MIL-STD-883 standards.

113

114 This paper presents a study of hermeticity and reliability aspects of laminates with membrane dies bonded  
115 by Al-Al thermocompression bonding, using different bonding parameters. An initial screening of the  
116 sealed dies was done after bonding by measuring their membrane deflection with white-light  
117 interferometry. A maximum leak rate (MLR) was estimated by measuring the membrane deflection at two  
118 different times. To look into some reliability aspects of the bonded laminates, a steady-state life-, a  
119 thermal shock- and a moisture resistance- test were performed. The bond strength of individual dies was  
120 estimated by measurements from shear test and pull test before and after the environmental stressing.

121

122 **Experimental**

123

124 Wafer design

125

126 Top Si wafers (150 mm) consisting of cavities with pressure-sensitive membranes were bonded to bottom  
127 Si wafers with bond frames of different widths. The wafers with cavities had 481 square membrane  
128 structures with a nominal thickness of 36 μm and a nominal side edge length of 2.5 mm. Pressure  
129 sensitive membranes deflect depending on the pressure difference between the inside and the outside of  
130 the cavity. The relation between the pressure difference and deflection is given by the following  
131 equation.<sup>9</sup>

132

133

$$w = (a^4 * (1 - \nu^2) * \Delta P) / (66 * d^3 * E) \quad [1]$$

134

135 Here,  $w$  is the deflection,  $a$  is the membrane side edge length,  $d$  is the membrane thickness,  $\nu$  is the  
136 Poisson's ratio,  $E$  is the Young's modulus, and  $\Delta P$  is the pressure difference.

137

138 The bottom wafers were designed to have 3  $\mu\text{m}$  high protruding frame structures of width 20, 40, 80 and  
139 200  $\mu\text{m}$ , which defined the bonding area. All frame designs had rounded corners, but a version with  
140 square corners was added with a 40  $\mu\text{m}$  wide frame, see Figure 1. Also one design of each frame width  
141 having a 200  $\mu\text{m}$  gap in the sealing frame at two different positions was added in order to have a few  
142 intentionally unsealed cavities for reference purposes. All frame structures had inner dimensions of 3.3  
143  $\text{mm} \times 3.3 \text{ mm}$ . The various designs were distributed evenly across the wafer. The total bonding area of all  
144 bond frames on a 150 mm wafer was 590  $\text{mm}^2$ . The number of dies of each frame type, their description  
145 and their nominal bond areas are listed in Table I.

146

#### 147 Laminate preparation

148

149 Laminates were prepared by bonding top Si wafers containing membrane structures with bottom Si  
150 wafers containing frame structures. Eight laminates were prepared, see Table II. The thickness of the top  
151 wafers was 280  $\mu\text{m}$ . The membrane structures in the top wafers were made using tetra-methyl ammonium  
152 hydroxide (TMAH) etching. A 750 nm layer of thermal  $\text{SiO}_2$  was used as masking material and the mask  
153 was not removed after the etching. The remaining layer of  $\text{SiO}_2$  on the front side of the wafer was  
154 patterned for die numbering. The membranes were fully covered by  $\text{SiO}_2$  on the resulting outside. The  
155 bottom wafers with frame structures were 400  $\mu\text{m}$  thick. The structures were made by etching 3  $\mu\text{m}$  into  
156 the silicon using deep reactive ion etching (DRIE) in an AMS 200 I-Prod (Alcatel). A thermal  $\text{SiO}_2$  of  
157 150 nm was used as masking material for this etching process. The mask was not removed after the  
158 etching. Before bonding, a layer of 1  $\mu\text{m}$  thick pure Al (99.999 %) was sputter deposited on all the top  
159 and bottom wafers. For the bottom wafers with protruding structures, the Al was left unpatterned. On the  
160 top wafers containing membranes, the Al was patterned, leaving Al only in the bond frame areas. The Al  
161 frames patterned on the top wafers were 40  $\mu\text{m}$  wider than their corresponding protruding bond frame  
162 structure on the bottom wafers. The advantage was a tolerance for a certain misalignment during bonding.  
163 Figure 2 shows a schematic cross-section of a bonded die.

164

#### 165 Bonding

166

167 The wafers were aligned in an EVG 620 bond aligner and bonded in an EVG 510 wafer bonder. The  
168 wafers were kept in place separated by spacers in the bonder after alignment. The ambient pressure of the  
169 bonding chamber was reduced to below  $1 \times 10^{-3}$  mbar before the spacers were removed. An initial bond  
170 force of 1 kN was applied and the temperature of the bonder was raised to the desired value, after which  
171 the specified bond force was applied. The thermocompression bonding was performed by applying a bond  
172 force of 36 or 60 kN at bonding temperatures of 300–400  $^\circ\text{C}$  for bonding durations of 15, 30, or 60  
173 minutes. An overview of the bonding parameters of the 8 bonded laminates is given in Table II. During  
174 the subsequent cool down, the bond force was reduced to 1 kN and was removed after the bonding tool  
175 temperature was below 50  $^\circ\text{C}$ .

176 The applied bond forces corresponded to bond pressures of 61 and 102 MPa. These pressure values are  
177 given just as a rough estimate and assume a perfectly stiff material (rigid body) with parallel surfaces. It  
178 should be noted that the actual local pressure can have non- uniformities that are pattern dependent caused  
179 by the pressure loading properties of the bonding chuck, pressure diffuser and the silicon wafer.<sup>10</sup>  
180 Additionally, the roughness and waviness of the surfaces will also cause the contact pressure to vary. It is  
181 still desirable to make comparisons between the different frame sizes (Table I), for which the difference  
182 in the contact pressure of different frames should be considered. We have chosen to roughly estimate the  
183 contact pressure of each bonding frame ( $\sigma_b$ ) by the simple expression.

$$\sigma_b = A_d * F_{tool} / A_o * A_{bf} = 1.55 \times 10^{-3} F_{tool} / A_{bf} \quad [2]$$

186  
187 Here,  $F_{tool}$  is the applied force of the bonding tool (36 kN or 60 kN),  $A_{bf}$  is the nominal bonding area of the  
188 particular frame (see Table I),  $A_d$  is the area of each die (5200×5200 μm), and  $A_o$  is the area of the Si  
189 wafer (0.01745 m<sup>2</sup>). This contact pressure is what one would have if each die was bonded separately as a  
190 rigid body with parallel surfaces under a pressure equal to the pressure on the whole wafer. This estimate  
191 ignores all horizontal components of stresses and maximizes the difference between the frame sizes.  
192 Using these simplifications, the calculated pressure on 20 μm wide frames is 214 MPa with 36 kN bond  
193 force and 357 MPa with 60 kN bond force. Similarly, the pressure on the 200 μm wide frames is 21 MPa  
194 with 36 kN bond force and 35 MPa with 60 kN bond force.

#### 195 Reliability tests

196  
197  
198 The laminates were stored for a minimum of 3 months after bonding and then diced along the diameter  
199 into two halves, each here called a half laminate. One half laminate of each Laminate ID in Table I was  
200 subjected to environmental stress tests consisting of a steady-state life test, a thermal shock test, and a  
201 moisture resistance test. The other half was kept as a reference.

202  
203 The first test was a steady-state life test in which the half laminates were exposed in an atmospheric  
204 ambient to 150 °C for 1000 hours in an oven (Heraeus Instruments). Secondly, the same half laminates  
205 were exposed to a thermal shock test where a two chamber system connected with a lift was employed  
206 (Heraeus HT7012 S2). The top chamber was maintained at a constant temperature of +200 °C and the  
207 bottom chamber was maintained at -65 °C. A dwell time in each chamber of 10 min and a transition time  
208 of ~7 s were employed. Consecutive exposure to both chambers was considered as 1 cycle and the  
209 samples were exposed for 50 cycles. Finally, the same half laminates were exposed to a moisture  
210 resistance test where a chamber with controlled humidity and temperature was used (Sunrise E series). A  
211 24 h initial conditioning of the samples at 80 °C was done to completely dry out the samples. One  
212 complete cycle comprised of 7 steps and the humidity of the chamber was maintained at 90 % for all the  
213 steps, as described in MIL-STD-883E. The temperature was varied between 25 °C to 65 °C during one  
214 cycle. The samples were exposed to 10 cycles. A subcycle of step 7 was performed for 5 of 10 cycles  
215 where humidity was uncontrolled and temperature was maintained at -10 °C (see MIL-STD-883E).

#### 216 Characterization

217  
218

219 The amount of inward deflection of bonded membranes was measured by a Zygo NewView 6300 white  
220 light interferometer (WLI). The deflection measurements were done on all dies, and were repeated after a  
221 period of 3–5 months. The hermetic yield was defined as the percentage of membranes deflecting inwards  
222 by more than 2  $\mu\text{m}$ . The open references were left out of the hermetic yield calculations. After  
223 environmental stressing, the membranes with inward deflection were identified by visual inspection and  
224 compared to a laminate map showing the membranes with inward deflection before environmental  
225 stressing.

226  
227 MLR was calculated by measuring the deflection of 1–13 membranes (for some laminates the target  
228 sample number, 13, was not available for testing) for each laminate at two different times  $t_1$  and  $t_2$ . Also  
229 the deflection of the membranes of the intentionally leaky dies was measured in order to measure possible  
230 deviations from a perfectly flat surface. MLR can be calculated by the following equation:

$$\text{MLR} = \Delta P * V / \Delta t \quad [3]$$

231  
232  
233  
234 Here,  $V$  is the cavity volume ( $\approx 1.6 \times 10^{-6}$  l),  $\Delta t$  is the time difference between times  $t_1$  and  $t_2$ , and  $\Delta P$  is  
235 the pressure difference in the cavity between times  $t_1$  and  $t_2$ . According to Equation 1, a deflection  
236 decrease of 0.45  $\mu\text{m}$  would correspond to a pressure increase of 65–99 mbar depending on the membrane  
237 thickness (ranged from 36.2–42.0  $\mu\text{m}$ , see Table III). In the calculation  $E = 165$  GPa and  $\nu = 0.28$  was  
238 used. Hence, if the measured deflection change was smaller than 0.45  $\mu\text{m}$ ,  $\Delta P$  is lower than 99 mbar.

239  
240 After environmental stressing, the two halves (stressed and un-stressed) of four laminates A400-60,  
241 B300-60, B350-15 and B400-60 were diced into individual dies. The dicing yield, defined as the  
242 percentage of dies that were not delaminated after the dicing process, was recorded.

243  
244 The dies which survived dicing test were used for the subsequent bond strength measurements. The shear  
245 strength was measured by shear testing of the individual dies. A random selection of 10 dies of frame type  
246 F80R was made from both the stressed and unstressed halves. Selected dies were glued to a flat sample  
247 holder and shear tested using a Dage 4000 PLUS multipurpose bond tester. The time versus applied mass  
248 [kg] was recorded and the mass at which the first fracture occurred, designated as the fracture mass, was  
249 noted. The shear strength [MPa] was calculated by multiplying the fracture mass by the gravitational  
250 constant and dividing by the nominal bond area.

251  
252 Similarly, the tensile strength was measured by pull testing of the individual dies. A random selection of  
253 10 dies of frame type F40R was made from both the stressed and unstressed halves. Also, 15 dies of  
254 frame types F20R, F40, F80R and F200R were randomly selected from B350-15 stressed half laminate.  
255 Selected dies were glued to flat headed bolts and pull tested using a MiniMat2000 (Rheometric Inc.). The  
256 elongation versus applied force was recorded and the force at which the fracture occurred, designated as  
257 the fracture force, was noted. The tensile strength [MPa] was calculated by dividing the fracture force by  
258 the nominal bond area.

259  
260 **Results**

261

262 Inward deflection of the membranes of sealed cavities (caused by the difference in pressure outside and  
263 inside the cavity) was observed directly after bonding. A typical picture of a bonded laminate is shown in  
264 Figure 3. The measured actual membrane thickness, inward deflection of membranes and calculated  
265 values of  $\Delta P$  by Equation 1 are listed in Table III. The deflection measurements indicated that the  
266 laminate B400-60 had the lowest pressure and laminate A400-60 had the highest pressure inside the  
267 sealed cavity. No significant difference in cavity pressure was observed for the other laminates. After a  
268 storage period of 3–5 months, a positive average change of  $\sim 0.1 \pm 0.05 \mu\text{m}$  in membrane deflection was  
269 observed for all laminates. Using an over-estimate for the maximum change in deflection of  $0.45 \mu\text{m}$ , an  
270 MLR value was calculated by Equation (3) and is listed in Table III. The difference in the MLR values  
271 only reflects the difference in storage times. The MLR was in the  $10^{-11}$ – $10^{-12} \text{ mbar}\cdot\text{l}\cdot\text{s}^{-1}$  range for all  
272 laminates. There were no systematic differences in MLR for laminates bonded with different bonding  
273 parameters. Also there was no systematic difference in leak rates between the different frame widths.  
274 Almost 85 % of the intentionally unsealed dies were deflecting upwards while only 15 % of them were  
275 still deflecting downwards. An average upward deflection of  $0.2 \pm 0.1 \mu\text{m}$  was observed for the  
276 intentionally unsealed dies.

277  
278 The hermetic yield results of all bonded laminates are shown in Table II and Figure 4. Laminate B350-15,  
279 bonded applying a bond force of 60 kN at a bonding temperature of  $350 \text{ }^\circ\text{C}$  for 15 minutes, had the  
280 highest hermetic yield of 92.6 %. Laminates B350-60 and B400-15 had a hermetic yield below 65 %, but  
281 the reason for their low yield was identified as misalignment of the wafers; the widest frame design (200  
282  $\mu\text{m}$ ) of these laminates had almost 100 % yield while the narrower frames had lower yield. In addition,  
283 misalignment was observed in studies of cross sections of the laminates. On the other hand, laminates  
284 A350-30, A400-60 and B300-60 showed a low hermetic yield too, without any clear evidence of  
285 misalignments. This indicated that a bond force of 36 kN or a bonding temperature of  $300 \text{ }^\circ\text{C}$  was not  
286 sufficient to provide a tight seal across the entire laminate. The results show that the laminates bonded at  
287 a bonding temperature  $\geq 350 \text{ }^\circ\text{C}$  applying a bond force of 60 kN for at least 15 minutes (i.e. B350-15 to  
288 B400-60) had a high hermetic yield (except the misaligned ones). The hermetic yield for the different  
289 frame types of laminates with an overall hermetic yield above 75 %, i.e. B350-15, B350-30 and B400-60,  
290 is shown in Figure 5. Frame type F40, F40R and F80R had high hermetic yield for all laminates, while  
291 F20R and F200R frame types had low hermetic yield for at least one laminate.

292  
293 After the steady-state life test, no membrane which had an inward deflection prior to stressing had turned  
294 flat. All laminates also survived the thermal shock test; dies that had deflecting membranes prior to this  
295 test, still had deflecting membranes after the thermal shock test. However, after the moisture resistance  
296 test, some dies that were originally deflecting, had turned flat. Figure 6 shows the percentage of dies that  
297 turned flat due to the moisture resistance test for the different laminates. For laminate A350-30, 11.1 % of  
298 the dies were flat, and for laminate B350-30, 0.5 % of the originally deflecting dies were flat after the  
299 moisture resistance test. No correlation between frame type and die leakage was observed. Some of the  
300 dies with originally flat membranes (i.e. leaky dies) were observed to deflect upwards after the moisture  
301 resistance test as seen in Figure 7.

302  
303 The dicing yield results of the four diced laminates are shown in Figure 8 and 9. Figure 8 shows laminate  
304 halves that were not environmentally stressed, and Figure 9 shows laminate halves that were  
305 environmentally stressed. The Figures show that the dicing yield of laminates A400-60, B350-15 and

306 B400-60 was above 95 %, regardless of frame type. The unstressed laminate half of B300-60 had a dicing  
307 yield below 60 % for all frame types, while the stressed laminate half of B300-60 had a dicing yield  
308 above 65 % for all frame types. Hence, a higher dicing yield after exposure to the environmental tests was  
309 observed for laminate B300-60.

310  
311 The shear strengths of frame type F80R from four stressed and unstressed laminates are shown in Figure  
312 10. The mean shear strength of unstressed laminates ranged from 28–84 MPa, while the mean shear  
313 strength of stressed laminates ranged from 40–77 MPa. There was an increase of 56 MPa in shear strength  
314 for unstressed laminates when increasing the bonding temperature from 300 °C to 400 °C. However, from  
315 the strength measurements of the stressed laminates, the difference between the laminates bonded at the  
316 lower and the higher temperature was apparently reduced to 37 MPa. There was an increase of about 7  
317 MPa in the shear strength for unstressed laminates when increasing the bond force from 36 kN to 60 kN  
318 at 400 °C. The same delta in bond strength was measured for the stressed laminates. The mean shear  
319 strength of the unstressed half laminate bonded at 300 °C was 12 MPa lower than that of the stressed half  
320 laminate, but it was 7 MPa higher for the unstressed versus the stressed half laminate bonded at 400 °C.

321  
322 Figure 11 shows the pull test measurement results of frame type F40R from four stressed and unstressed  
323 laminates. The mean tensile strength of the unstressed laminates ranged from 40–186 MPa, while the  
324 mean tensile strength of the stressed laminates ranged from 64–190 MPa. There was an increase of about  
325 55 MPa in the tensile strength when increasing the bond force from 36 kN to 60 kN at 400 °C. The tensile  
326 strength of unstressed laminates was lower than the tensile strength of the stressed laminates for all  
327 bonding parameters and more so for the lower temperatures; for a bonding temperature of 300 °C, the  
328 tensile strength was apparently increased by 23 MPa after stressing whereas for the laminate bonded at  
329 400 °C an apparent increase of only 4 MPa was measured after stressing.

330  
331 The results of pull tested dies of all frame types from stressed half laminate B350-15 are shown in Figure  
332 12. Frame F200R had the highest fracture force of 82 N. Frames F40 and F40R had almost the same  
333 fracture force, while frame F20R had the lowest fracture force of 32 N. Bond frame 20R had the highest  
334 tensile strength of 124 MPa, while frame F200R had the lowest tensile strength of 31 MPa. Frames F40  
335 and F40R had the same tensile strength of 91 MPa.

## 336 337 **Discussion**

338  
339 From Figure 4 it can be seen that a bonding temperature of at least 350 °C was required to achieve sealed  
340 dies across the entire laminate. Laminate B300-60 bonded at 300 °C shows low hermetic yield, low  
341 dicing yield and the lowest tensile and shear strength, while laminate B350-15 bonded at 350 °C shows  
342 high hermetic yield, high dicing yield and higher tensile and shear strength. Our results indicate that there  
343 exists a threshold for the bonding temperature somewhere in the range between 300 and 350 °C. Dragoi et  
344 al.<sup>4</sup> reported a threshold in bonding temperature between 450 and 500 °C, but they applied a lower bond  
345 pressure. Dragoi et al.<sup>4</sup> used a bond pressure of 3.4 MPa and did not use an SiO<sub>2</sub> layer underneath  
346 bonding Al, while the bond pressure was estimated to be in the range of 21–357 MPa in our case, and we  
347 did have an SiO<sub>2</sub> underneath the bonding Al. These factors may account for the observed difference in the  
348 threshold temperature. An increase in the shear strength and tensile strength was observed for unstressed  
349 laminates with increase in bonding temperature, and the trend was still clearly measurable for the stressed



350 laminates. Bonding temperature is important for the diffusion of metal atoms across the bonding interface.  
351 The diffusion of Al atoms increase with increase in the bonding temperature. Increasing the bonding  
352 temperature also softens the Al material, which can increase the area in atomic contact between the  
353 surfaces to be bonded. Once the opposing bonding surfaces are in atomic contact, the diffusion of atoms  
354 across the interface makes the bond between them stronger.

355  
356 As seen from Figure 4, the bond force appeared to be critical and laminates bonded applying a bond force  
357 of 60 kN at 350 °C gave higher hermetic yield than laminates bonded applying 36 kN bond force at 350  
358 or 400 °C. Thus, a high hermetic yield was achieved at a reduced bonding temperature by increasing the  
359 bonding force. Also, an increase in shear and tensile strength was observed with increase in bond force  
360 from 36 kN to 60 kN at 400 °C. We think that the higher bond pressure helped in bringing the opposing  
361 bonding surfaces into intimate contact. In addition, the higher bonding pressure may assist in breaking the  
362 native oxide present on the Al surface. The native oxide is physically very strong<sup>11</sup> and may be broken by  
363 increasing the bond pressure. The hermetic yield results in Figure 4 give an indication of the minimum  
364 bonding force that is required to achieve a hermetic bond.

365  
366 The dicing yield results in Figures 8 and 9 show that a bonding temperature  $\geq 350$  °C was required to have  
367 a bond strong enough to survive the dicing process. This threshold temperature is the same as the  
368 threshold temperature required to obtain a high hermetic yield. The dicing yield of laminate A400-60,  
369 bonded applying a bond force of 36 kN, was 100 %. The shear and tensile strengths of A400-60 were  
370 higher than the laminates bonded at lower temperatures applying higher bond force, while its hermetic  
371 yield was lower than that of the other laminates. This result indicates that in the bond frames of laminate  
372 A400-60, there were enough contact points between the opposing Al surfaces to make the bond strong,  
373 but not hermetic. A higher bond force of 60 kN seems to have allowed contact between sufficient portions  
374 of the bonding surface to result in a hermetic bond. In Figure 8–11, it is seen that the dicing yield, shear  
375 strength and tensile strength of laminate B300-60 was increased after exposure to the environmental tests,  
376 while environmental stressing seemed to reduce or have no effect on the shear and tensile strengths of  
377 laminates bonded at higher temperatures. The reason for the increase in tensile strength of a weakly  
378 bonded laminate may be linked to grain boundary diffusion of Al atoms across the bonded interface,  
379 when annealing the laminate at 150 °C for 1000 h during the steady-state life test. There can be  
380 significant amount of grain boundary diffusion of Al atoms at low temperatures due to its low activation  
381 energy<sup>12</sup>, which can be responsible for the increase in bonding strength of a weakly bonded laminate.

382  
383 Figure 5 shows that frames F20R and F200R had lower hermetic yield for at least one laminate compared  
384 to the frames F40, F40R and F80R frame types. The low hermetic yield of the F20R frames, the  
385 narrowest frames, may be due to their limited tolerance for misalignment. The lower hermetic yield of  
386 F200R frame type may be due to the comparatively low local bond pressure because of the large frame  
387 area. A frame width in the range 40–80  $\mu\text{m}$  seemed to be suitable for MEMS device sealing given a  
388 traditional commercial wafer bonder with alignment precision in the range of  $\pm 5$ –10  $\mu\text{m}$ , as applied here.  
389 As seen from Figure 12, an increase in fracture force was observed with increasing bond frame area.  
390 Nevertheless, the calculated tensile strength decreased with increasing frame width, suggesting that the  
391 increase in fracture force was not proportional to the bond area.

392

393 Table III shows that the MLR of the bonded dies was in the range of  $10^{-11}$ – $10^{-12}$  mbar·l·s<sup>-1</sup> for all  
394 laminates. The actual leak rate of the bonds may be significantly lower, but a more precise estimate could  
395 not be made based on the applied method. In our work, the change in the membrane deflection measured  
396 at two different times was ~0.1 μm. Considering possible errors in the membrane thickness measurements,  
397 the varied WLI scan positions, and natural variations in the atmospheric pressure, a maximum change in  
398 membrane deflection was estimated to be 0.45 μm based on the following assumptions: A change in  
399 atmospheric pressure by 51 mbar would correspond to a change in membrane deflection by 0.3 μm, an  
400 error of 25 μm in measuring the same spot by WLI would correspond to a change in deflection by 0.05  
401 μm, and 0.1 μm was the measured change in deflection. Leak rates between  $10^{-11}$  and  $10^{-16}$  mbar·l·s<sup>-1</sup> are  
402 needed for various industrial applications.<sup>13</sup>

403

404 The slight bow observed for the intentionally leaky membranes is suspected to be related to thermo-  
405 mechanical stress built into the system during cool down from the bonding temperature caused by the  
406 difference in coefficient of thermal expansion of Al and Si. However, as seen from the environmental  
407 stress testing results, the bonds were strong enough to withstand the thermo-mechanical stress evolving  
408 during the thermal shock tests. On the other hand, leakage in dies was observed after the laminates had  
409 been exposed to the moisture resistance test. As seen from Figures 4 and 5, there was a correlation  
410 between a low hermetic yield and a high number of leaking dies. The cause of the leakage is under  
411 investigation. We expect that water molecules could have leaked into the originally leaky membranes  
412 during exposure to a high humidity at an elevated temperature. This could have caused membranes to  
413 deflect upwards after the test.

414

## 415 **Conclusion**

416

417 Hermeticity, reliability and strength of 8 laminates bonded by wafer-level Al-Al thermocompression  
418 bonding applying different parameters were investigated. All originally well bonded dies survived a  
419 steady-state life test and a thermal shock test, irrespective of bonding parameters, but leakage in 1–11% of  
420 the dies was observed after a moisture resistance test. Our results showed that a bond force of 60 kN and a  
421 bonding temperature of 350 °C kept for 15 min resulted in hermetic, reliable and strong bonds for more  
422 than 75 % of the dies on a 150 mm laminate. On the other hand, bonding at a temperature of 300 °C or  
423 applying only 36 kN bond force resulted in a lower hermetic yield and a higher risk for leakage after the  
424 moisture resistance test. The average bond strength of shear and pull tested dies from selected laminates  
425 was in the range of 28 to 190 MPa. The estimated maximum leak rate for all bonded laminates was in the  
426 range of  $10^{-11}$ – $10^{-12}$  mbar·l·s<sup>-1</sup>.

427

## 428 **Acknowledgments**

429

430 This work was supported by the Research Council of Norway through the MSENS project, contract No  
431 210601/O30. The authors wish to thank Astrid-Sofie Vardøy from SINTEF ICT for her extended help  
432 during reliability and shear tests.

433

434

435

436

437 **References**

438  
439  
440  
441  
442  
443  
444  
445  
446  
447  
448  
449  
450  
451  
452  
453  
454  
455  
456  
457  
458  
459  
460  
461  
462  
463  
464  
465  
466  
467  
468  
469  
470  
471  
472  
473  
474  
475  
476  
477  
478  
479  
480

1. M. Esashi , *J. Micromech. Microeng.*, **18**, 073001 (2008).
2. S. Farrens, *Proc.Mater.Res.Soc.Symp*, 1112-E01 (2008).
3. C. H. Yun, J. R. Martin, L. Chen and T. J. Frey, *ECS Trans.*, **16**, 8 (2008).
4. V. Dragoi, G. Mittendorfer, J. Buggraf and M. Wimplinger, *ECS Trans.*, **33**, 4 (2010).
5. J. Froemel, M. Baum, M. Wiemer, F. Roscher, M. Haubold, C. Jia and T. Gessner, *Transducers'11*, 990 (2011).
6. N. Malik, K. Schjølberg-Henriksen, E. Poppe, M.M.Visser Taklo and T.G. Finstad, *Sensor Actuat. A-Phys.*, **211**, 115 (2014).
7. Y. Tao and A. P. Malshe, *Microelectron. Reliab.*, **45**, 559 (2005).
8. S. Millar, M. P. Y. Desmulliez, *Sensor Review*, **29**, 4 (2009).
9. W.K. Schomburg, *Introduction to Microsystem Design*, Springer Berlin Heidelberg (2011).
10. C. H. Tsau, S. M. Spearing and M. A. Schmidt, *J. Microelectromech. Syst.*, **13**, 6 (2004).
11. A. Sverdlin, in *Handbook of Aluminum Volume 1 Physical Metallurgy and Processes*, G. E. Totten, Editors, p. 60, Marcel Dekker, Inc., New York (2003).
12. G. Stechauner and E. Kozeschnik, *CALPHAD*, **47**, 92-99 (2014).
13. S. Costello and M. P. Y. Desmulliez, in *Hermeticity Testing of MEMS and Microelectronic Packages*, p.63, Artech House, Norwood, Massachusetts (2013).

481 **Figure Captions**

482

483 Figure 1. The mask layout for the various frame designs of widths 20, 40, 80, and 200  $\mu\text{m}$ . In the lower  
484 left corner of each die there is a key describing the design. For F80R, "F" is for Frame, "80" is for 80  $\mu\text{m}$   
485 frame width, and "R" is for rounded corner.

486

487 Figure 2. Schematic cross-section of a bonded die. The top wafers contained membrane structures and the  
488 bottom wafers contained protruding frames.

489

490 Figure 3. Picture of the bonded laminate B300-60. The hazy spots on the laminate are the inward  
491 deflecting membranes. The wavy stripes are a mirror image of the laboratory ceiling, used to make the  
492 membrane deflection visible.

493

494 Figure 4. Hermetic yield based on inspection of 401 dies on 8 bonded laminates before environmental  
495 testing. The dashed line indicates 75% hermetic yield.

496

497 Figure 5. Hermetic yield for the different frame types for the three laminates B350-15, B350-30 and  
498 B400-60 before environmental testing. The dashed line indicates 75% hermetic yield.

499

500 Figure 6. Percentage of originally deflecting membranes that had turned flat after exposure to the  
501 moisture resistance test for all eight laminates.

502

503 Figure 7. The three black squares on right show the membranes that are deflecting upwards. These dies  
504 were identified as leaky and had a flat membrane before exposure to the moisture resistance test. Inset on  
505 left shows membrane deflecting inwards while inset on right shows membrane deflecting upwards.

506

507 Figure 8. Dicing yield of the four unstressed half laminates for the different bond frame designs. The  
508 dashed line shows a 90% dicing yield.

509

510 Figure 9. Dicing yield of the four stressed half laminates for the different bond frame designs. The dashed  
511 line shows a 90% dicing yield.

512

513 Figure 10. Mean shear strength and standard deviation of frame type F80R from four stressed and  
514 unstressed half laminates, calculated for minimum 6 dies. Prefix A in the name of laminate corresponds to  
515 a bonding force of 36 kN while prefix B corresponds to a bonding force of 60 kN.

516

517 Figure 11. Mean tensile strength and standard deviation of frame type F40R from four stressed and  
518 unstressed half laminates, calculated for minimum 6 dies. Prefix A in the name of laminate corresponds to  
519 a bonding force of 36 kN while prefix B corresponds to a bonding force of 60 kN.

520

521 Figure 12. Mean fracture force, mean tensile strength and their standard deviation from five different  
522 frame types of stressed half laminate B350-15. The results were calculated for minimum 7 dies. The mean  
523 tensile strength and its standard deviation are calculated by dividing the fracture force by the frame area.

524

525 **Table I.** Overview of chip designs. The number of dies is per wafer.

<b>Frame ID</b>	<b>Frame Description</b>	<b>Number of dies</b>	<b>Nominal bond area (mm<sup>2</sup>)</b>
F20R	Width 20 μm, rounded corners	79	0.26
F40	Width 40 μm, square corners	80	0.54
F40R	Width 40 μm, rounded corners	82	0.48
F80R	Width 80 μm, rounded corners	80	1.06
F200R	Width 200 μm, rounded corners	80	2.68
Open	Width 20,40,80 and 200 μm, opening in bond frame	4	0.25–2.6

526  
527  
528  
529  
530  
531  
532  
533  
534  
535  
536  
537  
538  
539  
540  
541  
542  
543  
544  
545  
546  
547  
548  
549  
550  
551  
552  
553  
554  
555  
556  
557  
558  
559  
560

561 **TABLE II.** Overview of laminate types, bond parameters and hermetic yield. The hermetic yield was  
 562 defined as the percentage of membranes deflecting inwards by more than 2  $\mu\text{m}$  after bonding, before  
 563 dicing, see the "Characterization" section. Laminate B350-60 and B400-15 were found to be misaligned.

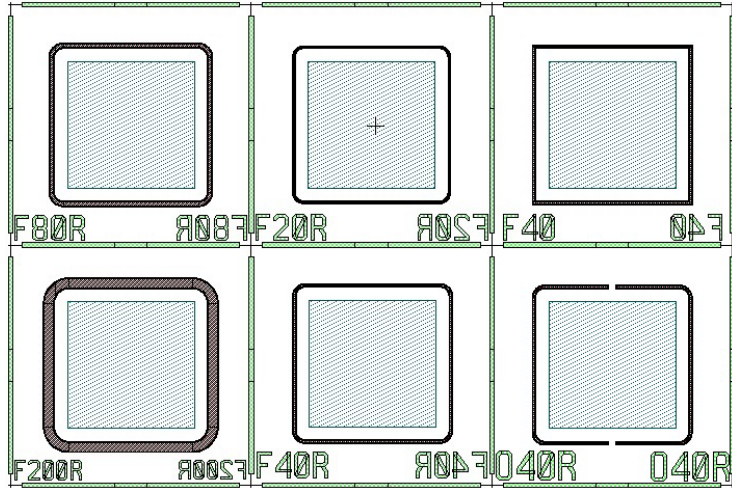
Laminate ID	Force (kN)	Temperature ( $^{\circ}\text{C}$ )	Time (minutes)	Hermetic Yield (%)
A350-30	36	350	30	11
A400-60	36	400	60	58
B300-60	60	300	60	64
B350-15	60	350	15	93
B350-30	60	350	30	80
B350-60	60	350	60	64
B400-15	60	400	15	44
B400-60	60	400	60	88

564  
 565  
 566  
 567  
 568  
 569  
 570  
 571  
 572  
 573  
 574  
 575  
 576  
 577  
 578  
 579  
 580  
 581  
 582  
 583  
 584  
 585  
 586  
 587  
 588  
 589  
 590  
 591  
 592

593 **TABLE III.** Measured membrane deflections and  $\Delta P$  as calculated from the inward membrane  
 594 deflections. The Max. Leak Rates were calculated based on various storage times.

Laminate ID	Membrane Thickness ( $\mu\text{m}$ )	Measured Deflection ( $\mu\text{m}$ )	$\Delta P$ Calculated from Deflection (mbar)	Max. Leak Rate ( $\text{mbar}\cdot\text{l}\cdot\text{s}^{-1}$ )
A350-30	40.5	5.1	1011	$1.3\times 10^{-11}$
A400-60	36.3	5.9	849	$1.4\times 10^{-11}$
B300-60	42	4.5	1003	$2.0\times 10^{-11}$
B350-15	36.6	7.0	1040	$1.5\times 10^{-11}$
B350-30	36.3	7.1	1027	$1.2\times 10^{-11}$
B350-60	36.4	7.4	1077	$9.6\times 10^{-12}$
B400-15	36.5	7.2	1062	$1.3\times 10^{-11}$
B400-60	36.2	7.7	1105	$1.6\times 10^{-11}$

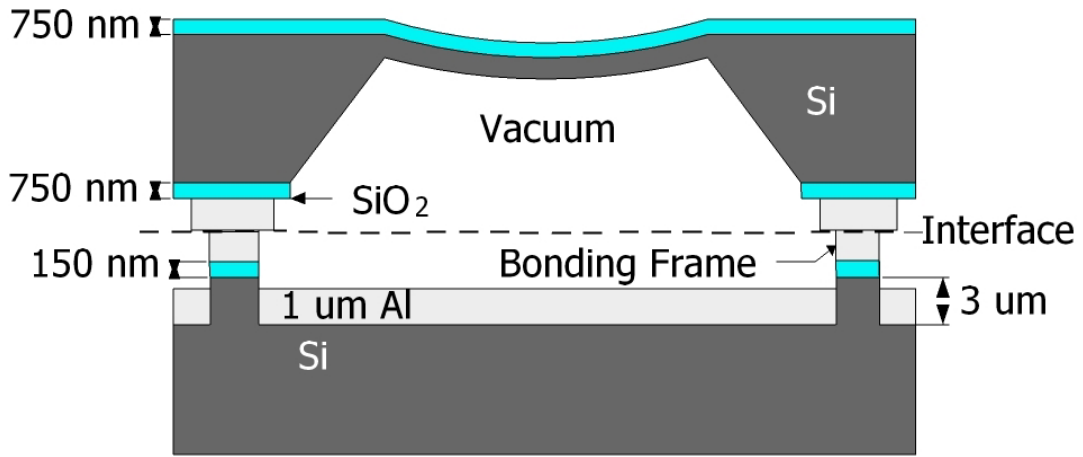
595  
 596  
 597  
 598  
 599  
 600  
 601  
 602  
 603  
 604  
 605  
 606  
 607  
 608  
 609  
 610  
 611  
 612  
 613  
 614  
 615



616  
 617  
 618  
 619  
 620  
 621  
 622  
 623  
 624  
 625  
 626  
 627  
 628  
 629  
 630  
 631  
 632  
 633  
 634  
 635  
 636  
 637

Figure 1. The mask layout for the various frame designs of widths 20, 40, 80, and 200  $\mu\text{m}$ . In the lower left corner of each die there is a key describing the design. For F80R, "F" is for Frame, "80" is for 80  $\mu\text{m}$  frame width, and "R" is for rounded corner.

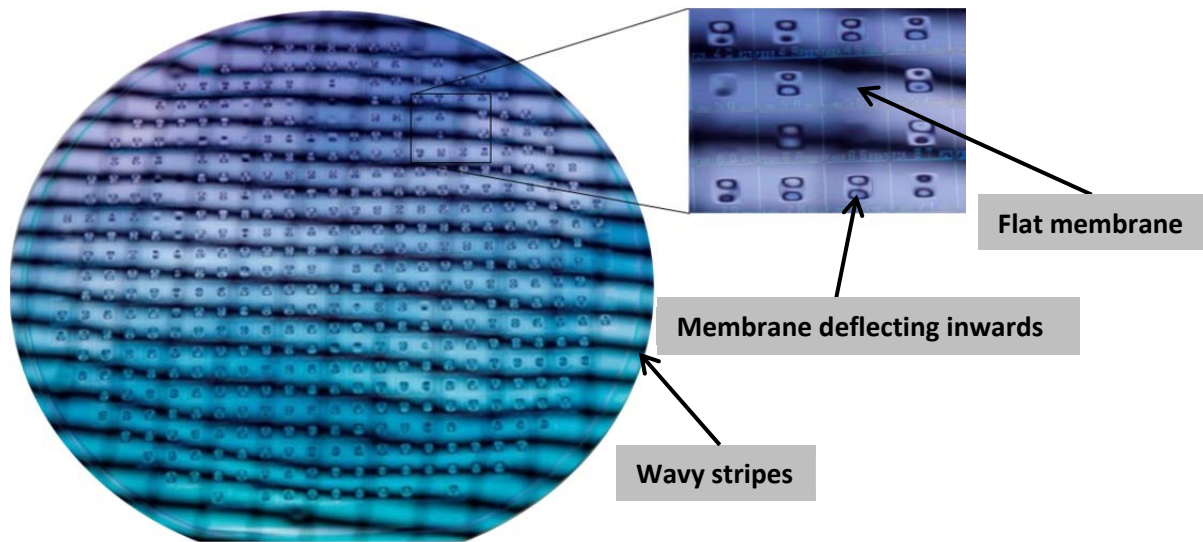




638  
 639 Figure 2. Schematic cross-section of a bonded die. The top wafers contained membrane structures and the  
 640 bottom wafers contained protruding frames.  
 641

642  
 643  
 644  
 645  
 646  
 647  
 648  
 649  
 650  
 651  
 652  
 653  
 654  
 655  
 656  
 657  
 658  
 659  
 660  
 661  
 662  
 663  
 664  
 665  
 666  
 667  
 668  
 669  
 670

671



672

673

674

675

676

677

678

679

680

681

682

683

684

685

686

687

688

689

690

691

692

693

694

695

696

697

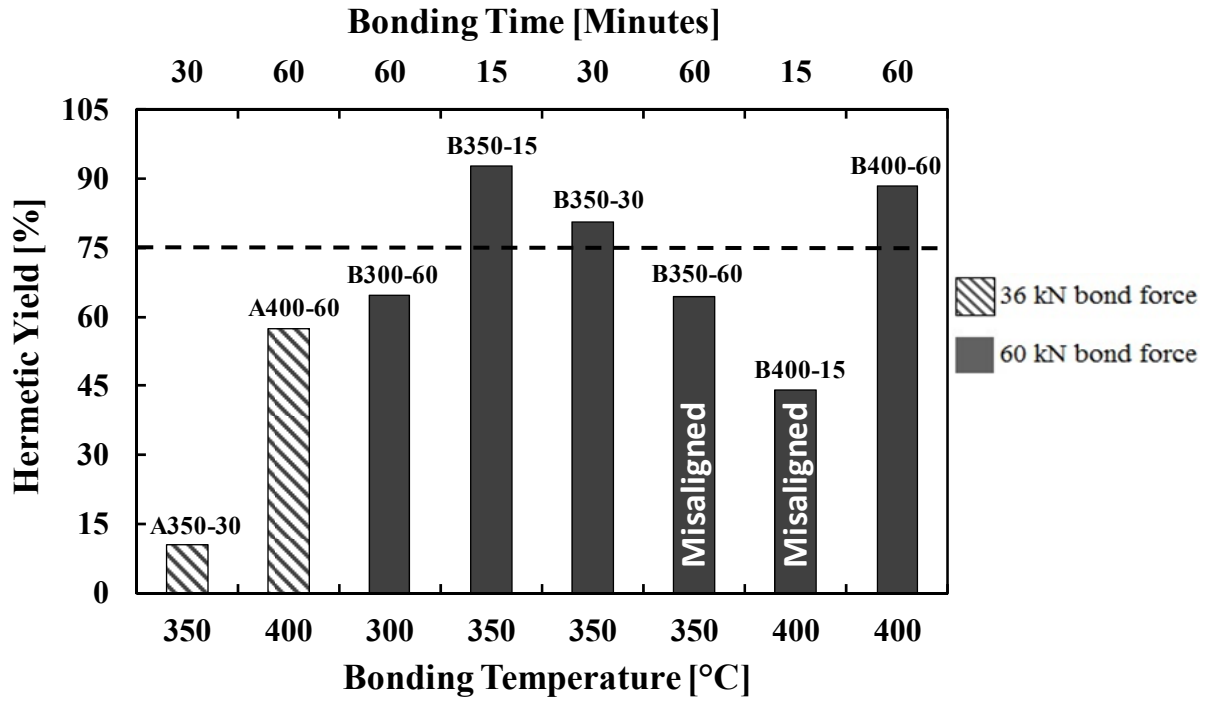
698

699

700

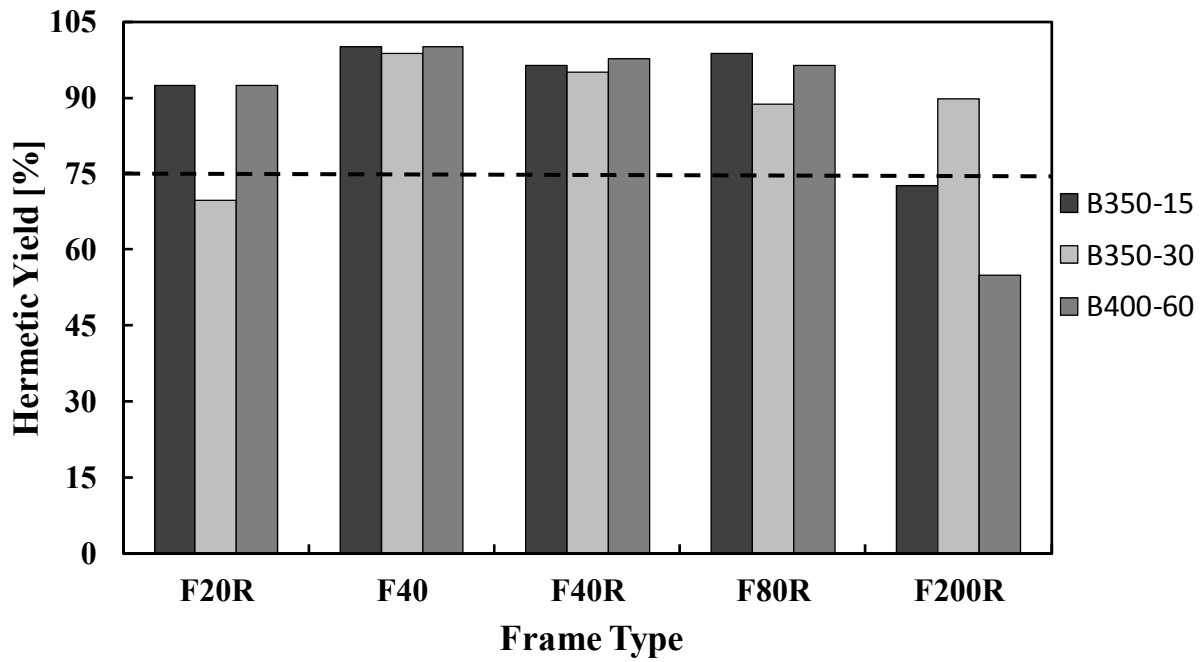
701

Figure 3. Picture of the bonded laminate B300-60. The hazy spots on the laminate are the inward deflecting membranes. The wavy stripes are a mirror image of the laboratory ceiling, used to make the membrane deflection visible.



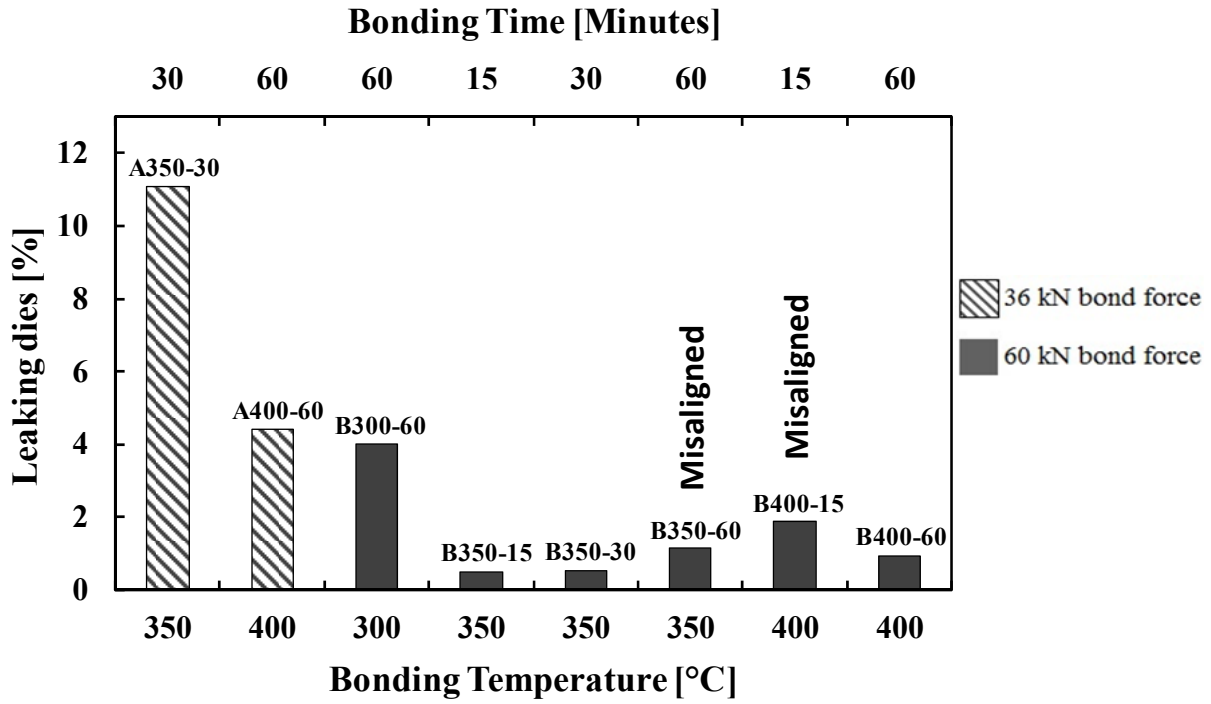
702  
703  
704  
705  
706  
707  
708  
709  
710  
711  
712  
713  
714  
715  
716  
717  
718  
719  
720  
721  
722  
723  
724  
725  
726  
727  
728

Figure 4. Hermetic yield based on inspection of 401 dies on 8 bonded laminates before environmental testing. The dashed line indicates 75% hermetic yield.



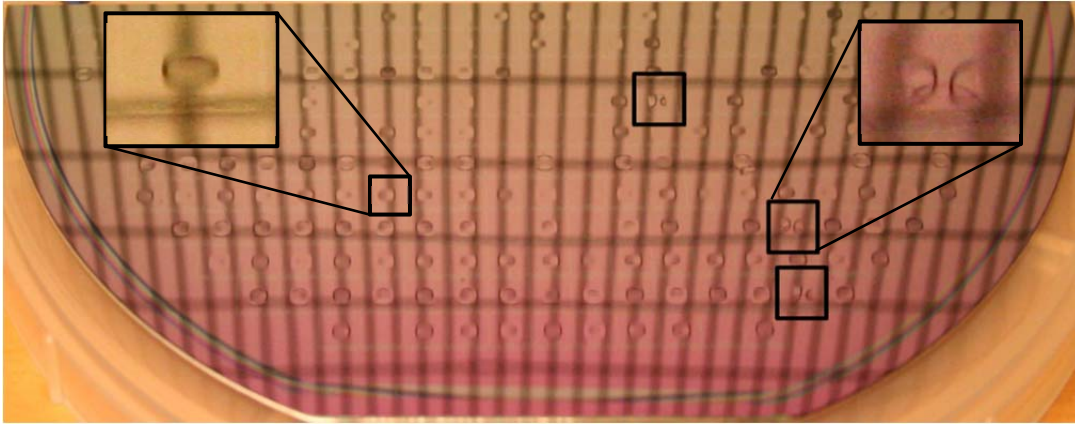
729  
 730  
 731  
 732  
 733  
 734  
 735  
 736  
 737  
 738

Figure 5. Hermetic yield for the different frame types for the three laminates B350-15, B350-30 and B400-60 before environmental testing. The dashed line indicates 75% hermetic yield.



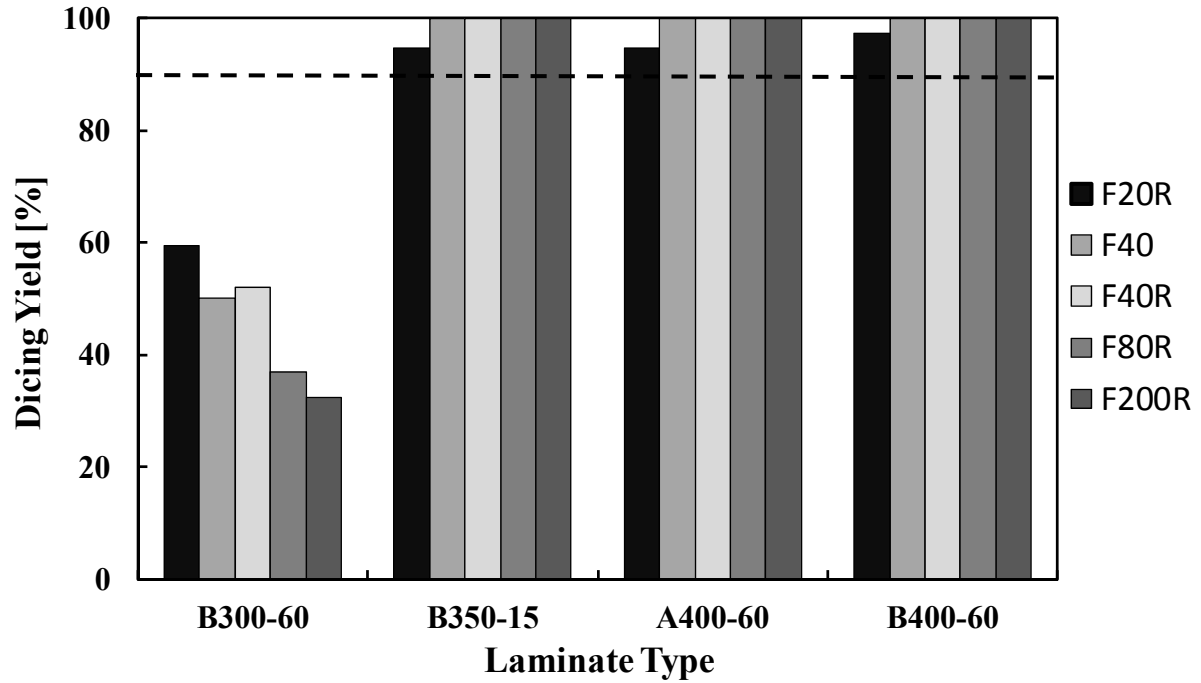
739  
 740  
 741  
 742  
 743  
 744  
 745  
 746  
 747  
 748  
 749  
 750  
 751  
 752  
 753  
 754  
 755

Figure 6. Percentage of originally deflecting membranes that had turned flat after exposure to the moisture resistance test for all eight laminates.



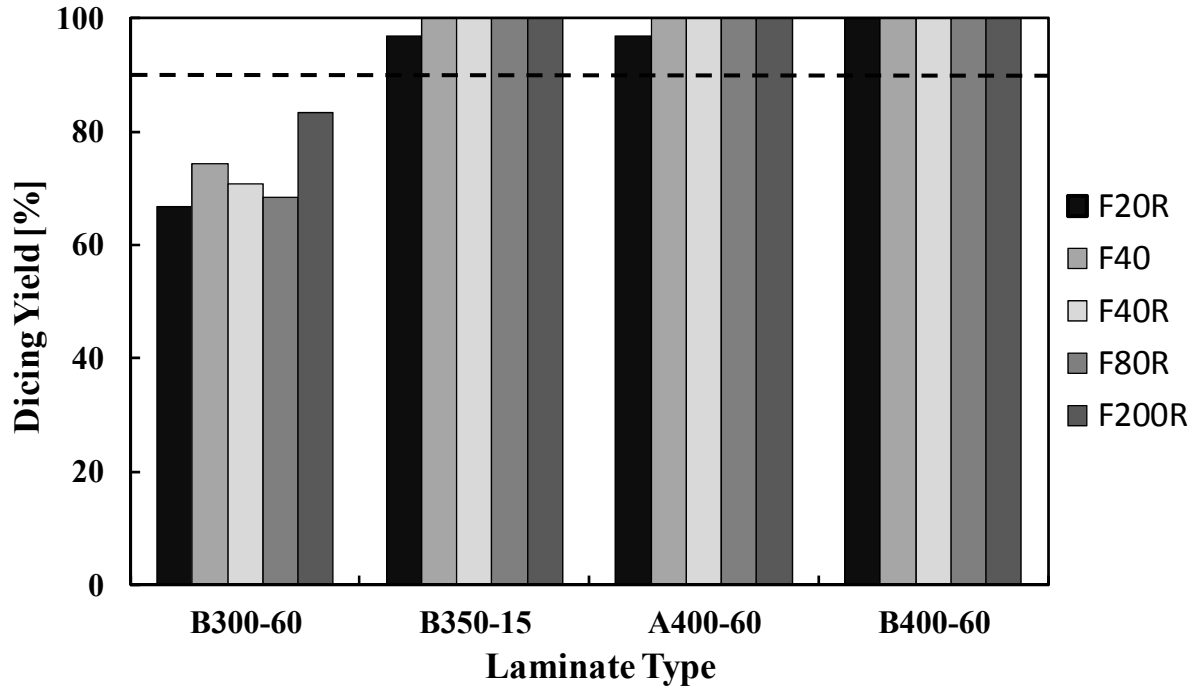
756  
757 Figure 7. The three black squares on right show the membranes that are deflecting upwards. These dies  
758 were identified as leaky and had a flat membrane before exposure to the moisture resistance test. Inset on  
759 left shows membrane deflecting inwards while inset on right shows membrane deflecting upwards.

760  
761  
762  
763  
764  
765  
766  
767  
768  
769  
770  
771  
772



773  
 774  
 775  
 776  
 777  
 778  
 779  
 780  
 781  
 782

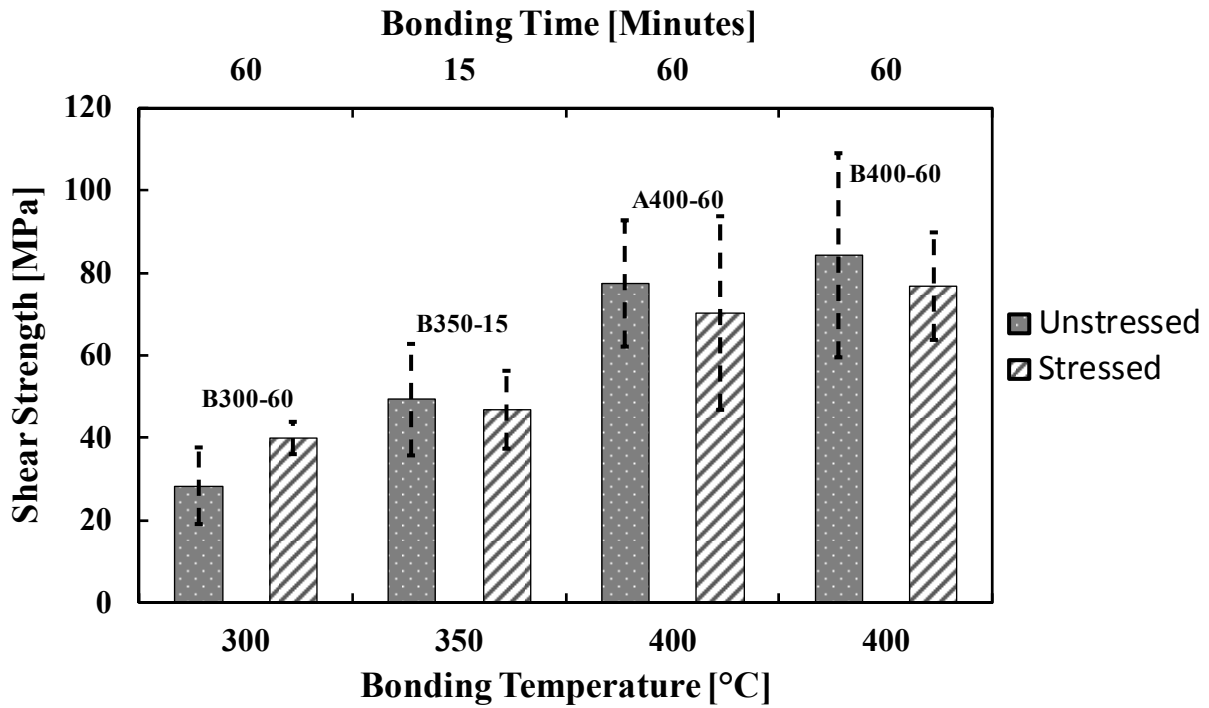
Figure 8. Dicing yield of the four unstressed half laminates for the different bond frame designs. The dashed line shows a 90% dicing yield.



783  
 784  
 785  
 786  
 787  
 788  
 789  
 790  
 791

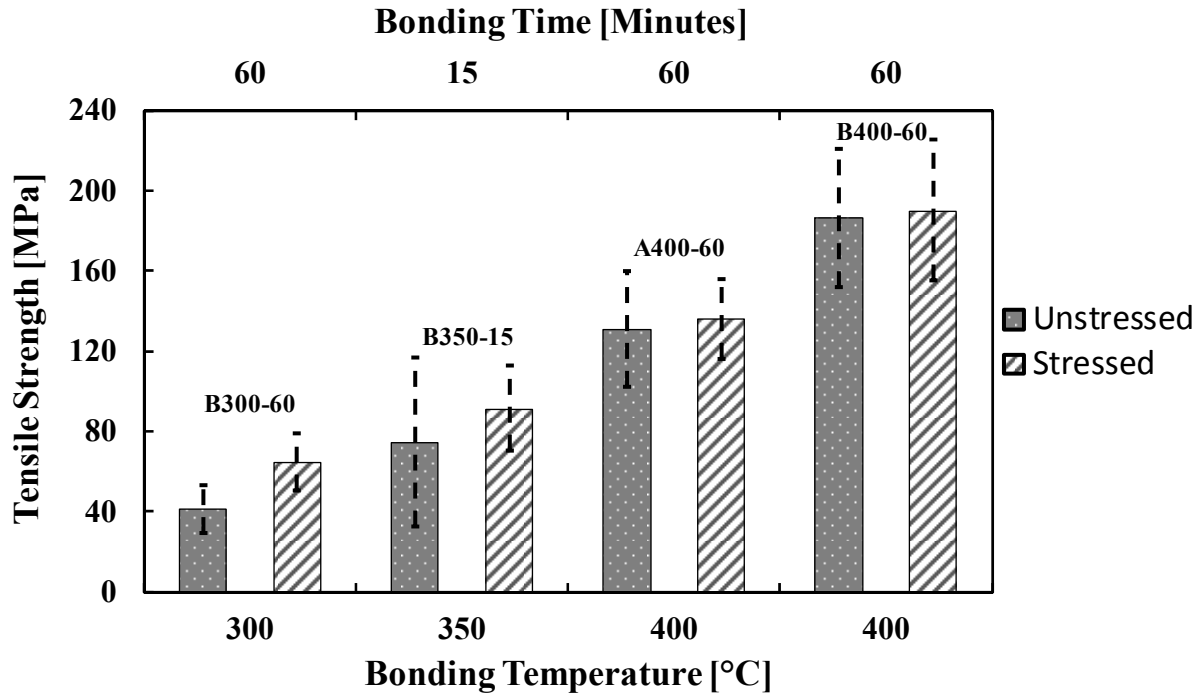
Figure 9. Dicing yield of the four stressed half laminates for the different bond frame designs. The dashed line shows a 90% dicing yield.





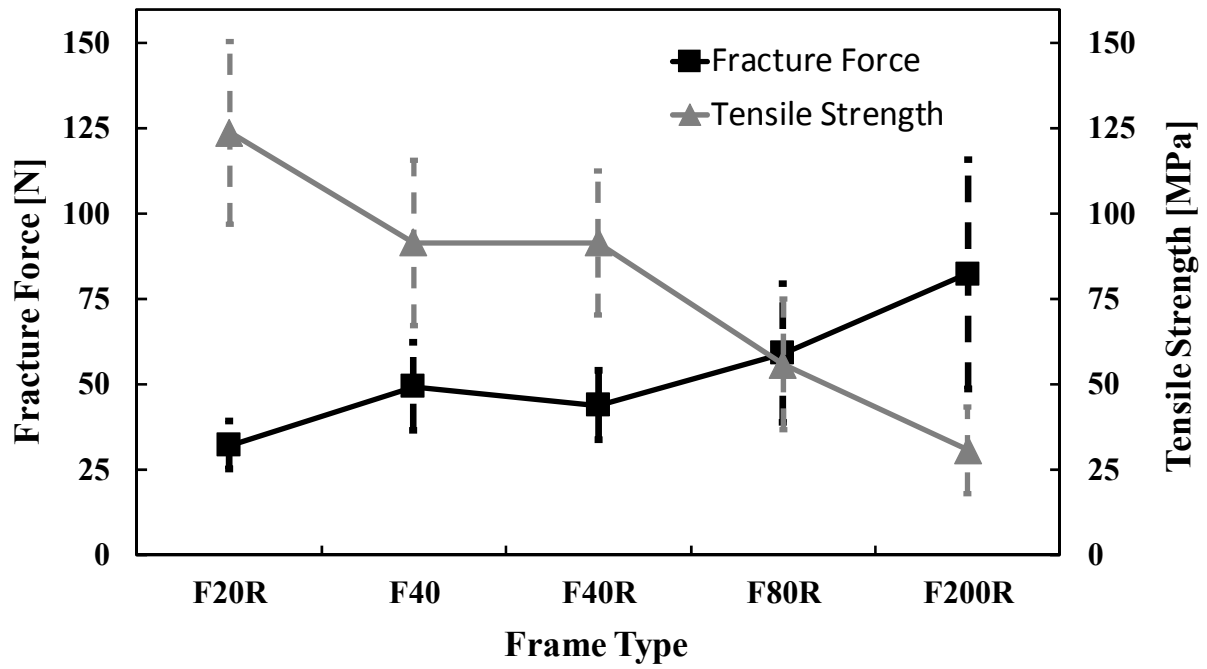
792  
793  
794  
795  
796  
797  
798  
799  
800  
801

Figure 10. Mean shear strength and standard deviation of frame type F80R from four stressed and unstressed half laminates, calculated for minimum 6 dies. Prefix A in the name of laminate corresponds to a bonding force of 36 kN while prefix B corresponds to a bonding force of 60 kN.



802  
803  
804  
805  
806  
807  
808  
809  
810  
811  
812  
813  
814  
815  
816  
817  
818  
819  
820

Figure 11. Mean tensile strength and standard deviation of frame type F40R from four stressed and unstressed half laminates, calculated for minimum 6 dies. Prefix A in the name of laminate corresponds to a bonding force of 36 kN while prefix B corresponds to a bonding force of 60 kN.



821  
 822 Figure 12. Mean fracture force, mean tensile strength and their standard deviation from five different  
 823 frame types of stressed half laminate B350-15. The results were calculated for minimum 7 dies. The mean  
 824 tensile strength and its standard deviation are calculated by dividing the fracture force by the frame area.